RESEARCH ARTICLE

Nucleotide sugar biosynthesis occurs in the glycosomes of procyclic and bloodstream form *Trypanosoma brucei*

Maria Lucia Sampaio Guther[1], **Alan R. Prescott**[2], **Sabine Kuettel**[1], **Michele Tinti**[1], **Michael A. J. Ferguson**[1] *

1 Wellcome Centre for Anti-Infectives Research, School of Life Sciences, University of Dundee, Dundee, United Kingdom, 2 Dundee Imaging Facility, School of Life Sciences, University of Dundee, Dundee, United Kingdom

* m.a.j.ferguson@dundee.ac.uk

Abstract

In *Trypanosoma brucei*, there are fourteen enzymatic biotransformations that collectively convert glucose into five essential nucleotide sugars: UDP-Glc, UDP-Gal, UDP-GlcNAc, GDP-Man and GDP-Fuc. These biotransformations are catalyzed by thirteen discrete enzymes, five of which possess putative peroxisome targeting sequences. Published experimental analyses using immunofluorescence microscopy and/or digitonin latency and/or subcellular fractionation and/or organelle proteomics have localized eight and six of these enzymes to the glycosomes of bloodstream form and procyclic form *T. brucei*, respectively. Here we increase these glycosome localizations to eleven in both lifecycle stages while noting that one, phospho-N-acetylglucosamine mutase, also localizes to the cytoplasm. In the course of these studies, the heterogeneity of glycosome contents was also noted. These data suggest that, unlike other eukaryotes, all of nucleotide sugar biosynthesis in *T. brucei* is compartmentalized to the glycosomes in both lifecycle stages. The implications are discussed.

Author summary

All eukaryotes add sugar chains to proteins to make glycoproteins, most of which decorate the cell surface and play central roles in how cells interact with their environment and with other cells. These sugar chains are built up using nucleotide sugars to donate the individual sugars. The nucleotide sugars themselves are generally made in the cytoplasm of cells but in *Trypanosoma brucei*, the causative agent of human African trypanosomiasis and nagana in cattle, they are made inside small organelles called glycosomes. This very unusual arrangement in parasite metabolism is notable and may offer therapeutic opportunities.

Introduction

The tsetse-fly transmitted protozoan parasite *Trypanosoma brucei* is responsible for human and animal African trypanosomiasis. The bloodstream form (bsf) of this organism depends on

a surface coat made of glycosylphosphatidylinositol (GPI) anchored and *N*-glycosylated variant surface glycoprotein (VSG) to evade the host innate immune system and the acquired immune system through antigenic variation [1]. The bsf parasite also expresses many lower abundance glycoproteins, such as a novel transferrin receptor (TfR) [2–4], a lysosomal/endosomal protein called p67 [5], the invariant surface (ISG) and endoplasmic reticulum (IGP) glycoproteins [6,7], the Golgi/lysosomal glycoprotein tGLP-1 [8], the membrane-bound histidine acid phosphatase TbMBAP1 [9], the flagellar adhesion zone glycoproteins Fla1-3 [10,11], the flagellar pocket/endosomal system haptoglobin-hemoglobin receptor (HpHbr) [12] and serum resistance antigen (SRA) [13], the complement factor H receptor (FHR) [14] and others, such as the metacyclic trypomastigote-specific ISG [15]. Some of these are metacyclic and/or bsf specific glycoproteins (eg. VSG, TfR, ISG, TbMAP1, HpHbr, SRA, FHR) while others are also common to the tsetse midgut-dwelling procyclic form (pcf) of the parasite. Further, pcf parasites also express unique glycoproteins, notably the abundant GPI-anchored procyclins, some of which are *N*-glycosylated [16,17], and a high-molecular weight glycoconjugate [18,19]. Many of the *N*-glycan structures expressed by bsf *T. brucei* have been solved and these include conventional oligomannose and biantennary complex structures as well as paucimannose and extremely unusual 'giant' poly-*N*-acetyl-lactosamine (poly-LacNAc) containing complex structures [20–23]. In contrast, only oligomannose *N*-glycans have been structurally described in wild type pcf trypanosomes [16,24]. The GPI anchor structures of several bsf VSGs [25–28] and of the TfR [5,29] have also been solved, as have those of pcf procyclins [16]. Both bsf and pcf GPI anchors contain the canonical conserved GPI core structure but they are the most divergent among the eukaryotes in terms of their carbohydrate sidechains, containing up to 1 βGal and 5 αGal residues in the bsf GPI sidechains and multiple, branched, *N*-acetyllactosamine and lacto-*N*-biose repeats capped with α2–3 sialic acid in the pcf GPI sidechains [16,27,30,31]. Recently, the *O*-glycosylation (via novel Glcα1-*O*-Ser linkages) of certain VSG variants has also been described [32]. The entire repertoire of known *T. brucei N*-linked, *O*-linked and GPI glycans is composed exclusively of the monosaccharides mannose, galactose, glucose, N-acetylglucosamine, glucosamine and sialic acid. In addition, a trace of fucose has been reported in the pcf high-molecular weight glycoconjugate [19], and recent data suggest that fucosylation may occur inside the parasite mitochondrion [33]. These combined monosaccharide compositions are consistent with the nucleotide sugar biosynthetic capacity of bsf and pcf trypanosomes [34] (Fig 1), apart from the absence of CMP-sialic acid. However, this apparent discrepancy is because sialic acid is added to the procyclin GPI sidechains via cell-surface transialidase enzymes that transfer α2–3 sialic acid from host glycoconjugates in a nucleotide sugar-independent reaction [35,36]. The non-*N*-acetylated glucosamine in the GPI anchors originates from UDP-GlcNAc and is the product of the GPI pathway GlcNAc-PI de-*N*-acetylase [37,38]. Although mature *T. brucei N*-glycans do not contain glucose, the trypanosome *N*-glycans undergo reversible glucosylation from UDP-Glc in the endoplasmic reticulum (ER) as part of a UDP-Glc: unfolded glycoprotein glucosyltransferase (UGGT) / α-glucosidase II / calreticulin ER quality control system [23,39]. In *T. brucei* UDP-Glc is also the donor for the biosynthesis of base J [40], the obligate precursor of UDP-Gal (via UDP-Glc 4'-epimerase (TbGALE) [41]), and presumed to be the donor for VSG *O*-glycosylation [32].

Nucleotide sugar biosynthesis in *T. brucei* is quite conventional, in so far as homologues of most of the necessary enzymes can be found by BLASTp searches with corresponding prokaryotic and/or eukaryotic amino acid sequences [34]. The only exception to this is the absence of a canonical phosphoglucose mutase (PGM) enzyme, the function of which is redundantly replaced by the parasite phosphomannose mutase (TbPMM) and phospho-N-acetylglucosamine mutase (TbPAGM) enzymes [42]. Further, the following trypanosome enzymes of nucleotide sugar biosynthesis have been expressed in *E. coli* and shown, where determined, to have
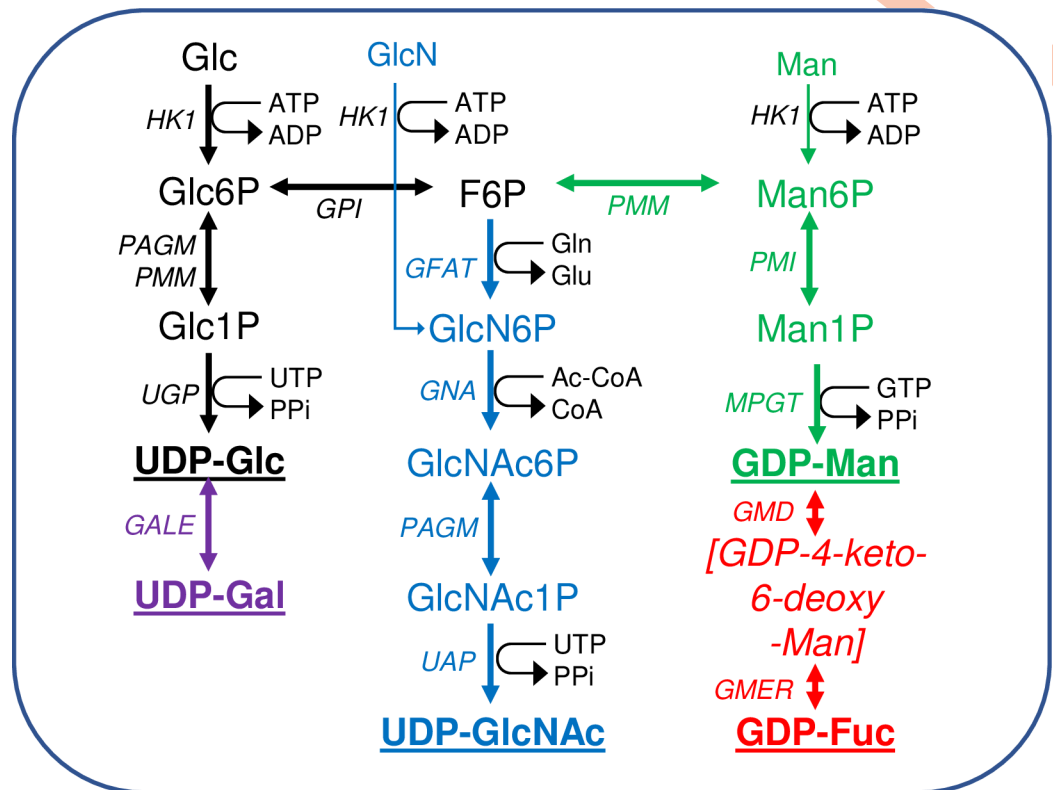
Fig 1. Scheme of nucleotide sugar biosynthesis in *T. brucei*. Nucleotide sugar biosynthesis in *T. brucei* according to [34], showing the 14 biotransformations and 13 enzymes involved. No dedicated phospho-glucose mutase (PGM) gene exists in T. brucei and the interconversion of Glc6P and Glc1P is performed by PAGM and/or PMM [42]. The enzyme abbreviations (*in italics*) appear in the Introduction. The terminal nucleotide sugars used for glycosylation reactions are in bold and underlined. Information on enzyme essentiality, protein and antibody production, and sub-cellular localisation appear in (Table 1). The main source of all of the nucleotide sugars is Glc but both Man and GlcN can enter their respective pathways via hexokinase (HK1).

https://doi.org/10.1371/journal.pntd.0009132.g001

typical kinetic properties and conserved three dimensional structures (Table 1): UDP-glucose 4'-epimerase (TbGALE) [43,44]. UDP-glucose pyrophosphorylase (TbUGP) [45]. Phospho-mannose isomerase (TbPMI) [46]. Phosphomannose mutase (TbPMM) [42,47]. Mannose phosphate guanyltransferase (TbMPGT) [47,48]. Glucosamine-6-phosphate N-acetyltransfer-ase (TbGNA) [49]. Phospho-N-acetylglucosamine mutase (TbPAGM) [42]. UDP-N-acetylglu-cosamine pyrophosphorylase (TbUAP) [50,51]. GDP-mannose dehydratase (TbGMD) [52]. GDP-4-dehydro-6-deoxy-D-mannose epimerase/reductase (TbGMER) [52]. However, where nucleotide sugar biosynthesis in *T. brucei* diverges most dramatically from the norm is with respect to its subcellular location. Thus, whereas eukaryotic nucleotide sugar biosynthesis is generally either known or assumed to occur in the cytoplasm, for *T. brucei* many of these reactions appear to occur in the glycosomes [42,44–46,49,50,52–54] (Table 1). Glycosomes are kinetoplastid peroxisome-like membrane-bound organelles, named such because they contain enzymes of glycolysis [55–59,66–68], including hexokinase (TbHK1) and phospho-glucose isomerase (TbPGI) that are also components of the *de novo* pathways to the nucleotide sugars.

Here, we analyse the subcellular locations of nine nucleotide sugar biosynthetic enzymes in pcf trypanosomes by immunofluorescence microscopy using mono-specific mouse polyclonal antibodies raised to purified recombinant, soluble and enzymatically active proteins. Further, we use eight of these nine antibodies to determine the digitonin latency of the corresponding

Glycosomal nucleotide sugar synthesis in *T. brucei*

Table 1. Summary of data on *T. brucei* nucleotide sugar biosynthetic enzymes. Data from the literature [#] are in black, data from this paper [TP] are in red. GL = glycosomal; CP = cytoplasmic; IFM = immunofluorescence microscopy; *indicates that IFM was performed using an epitope tag rather than an antibody to the whole protein; PTS = peroxisome targeting sequence (type 1 or type 2) for the respective *T. brucei* (Tb), *T. cruzi* (Tc) and *L. major* (Lm) enzymes [50,65]. Enzyme abbreviations are listed in the Introduction, with the exception of TbGFAT, glutamine: fructose-6-phosphate aminotransferase.

Essential		Protein expression, crystallography and antibodies			IFM		Digitonin Latency		Sub-cellular fractionation		Glycosome proteome				PTS
Enzyme	Gene	bsf	pcf	Prot	Xtal	Ab	bsf	pcf	bsf	pcf	bsf	pcf	bsf	pcf	Tb Tc Lm
TbHK1	Tb927.10.2010	[62,63]		[60]		[59]	GL [59]	GL [59]	GL [58,59]	GL [57,59]	GL [55,56]	GL [57,58]	GL [53]	GL [54, TP]	2 2 2
TbPGI	Tb927.1.3830			[64]	[64]				GL [59]		GL [55,56]	GL [57]		[53,54, TP]	1 1 1
TbUGP	Tb927.10.13130	[45]		[45]	[45]	[45]	[45]	GL [TP]	GL [TP]	GL [TP]	GL [TP]			GL [54]	1
TbGALE	Tb927.11.2730	[41]	[44]	[41]	[43]	[44, TP]	GL [44]	GL [44,TP]	GL [TP]	GL [TP]	GL [44]			GL [54]	1 2
TbGFAT	Tb927.7.5560														
TbGNA	Tb927.11.11100	[49]		[49]	[49]	[49]	GL [49]	GL [TP]							
TbPAGM	Tb927.8.980	[42]		[42]		[42]	GL [42]	GL+CP [TP]	GL+CP [42]	GL+CP [TP]					
TbUAP	Tb927.11.2520	[50]		[50]	[50]	[50, TP]	GL [50]	GL [TP]	GL [TP]	GL [TP]				GL [54]	1 1 1
TbPMI	Tb927.11.14780	[46]		[46]		[46]	GL [46]	GL [TP]	GL [TP]	GL [TP]	GL [TP]			GL [53,54, TP]	1 1
TbPMM	Tb927.10.6440	[42]		[42]	[42]	[42]	GL [42]	GL [TP]	GL [42,TP]	GL [TP]					1 1
TbMPGT	Tb927.8.2050	[47]		[47,48,TP]		[TP]	CP [48]	GL [TP]	GL [TP]	GL [TP]	CP [48]	GL [TP]			
TbGMD	Tb927.10.15490	[52]	[52]	[52]			GL [52]*								
TbGMER	Tb927.11.13990			[52]		[TP]	GL [TP]	GL [TP]	GL [TP]						

enzymes in both pcf and bsf trypanosomes. In addition, we localise three representative NS biosynthetic enzymes (TbPMI, TbMPGT and TbUGP) to the glycosome-containing small granular fraction by subcellular fractionation, and demonstrate heterogeneity in glycosome composition by density gradient centrifugation and proteomics.

Results

Subcellular localization by immunofluorescence microscopy

In previous work, we have purified the following soluble, enzymatically active, recombinant nucleotide sugar biosynthetic enzymes: TbUGP, TbGALE, TbGNA, TbPAGM, TbUAP, TbPMI and TbPMM (Table 1). With these, we have prepared either rabbit (TbGALE) or mouse polyclonal antibodies for immunofluorescence microscopy (IFM) localization studies against bsf trypanosomes (Table 1). To these we have added new polyclonal mono-specific mouse antibodies to recombinant TbGALE, TbGNA, TbUAP, TbMPGT and TbGMER (see Methods). In all cases, the mouse antibodies were affinity-purified against immobilized immunogen and/or demonstrated to be mono-specific by Western blotting (Table 2; S2 Fig). These antibodies were used in immunofluorescence microscopy against fixed and permeabilized pcf

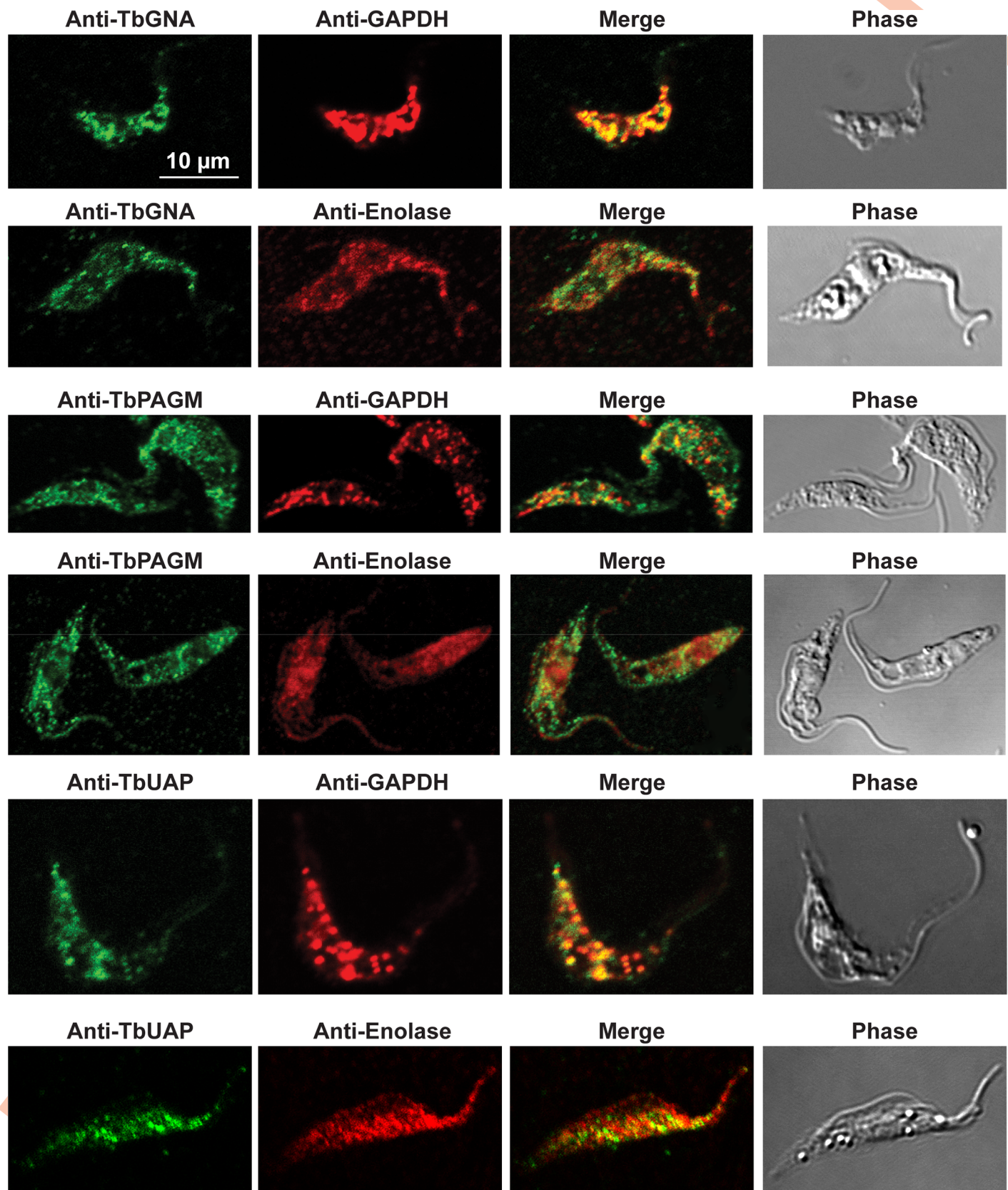**Table 2. Antibodies to nucleotide sugar biosynthetic enzymes used in this study.** [TP] = this paper.

Enzyme	Antibody species	Affinity purified	Mono-specific by Western	Reference
TbUGP	Mouse	Yes	Yes	[45]
TbGALE	Mouse	No	Yes	[TP]
TbGNA	Mouse	Yes	Yes	[TP]
TbPAGM	Mouse	No	Yes	[42]
TbUAP	Mouse	Yes	Yes	[TP]
TbPMI	Mouse	No	Yes	[46]
TbPMM	Mouse	No	Yes	[42]
TbMPGT	Mouse	No	Yes	[TP}
TbGMER	Mouse	No	Yes	[TP]

https://doi.org/10.1371/journal.pntd.0009132.t002

trypanosomes, along with rabbit antibodies to definitive glycosomal (TbGAPDH) and cytosolic (TbEnolase) markers (Figs 2, 3, and 4). Wider field images containing several cells are available in (10.6084/m9.figshare.13124909). In all cases, except for TbPAGM (Fig 2, middle panels), the mono-specific mouse antibodies produced punctate staining that was coincident, at least in part, with the rabbit anti-TbGAPDH antibody staining, suggesting glycosomal locations. In contrast, there was no overlap with cytoplasmic anti-TbEnolase immunostaining. In the case of TbPAGM, the immunostaining suggested both glycosomal and cytosolic localization. Interestingly, the punctate co-staining with anti-NS biosynthetic enzyme and anti-TbGAPDH antibodies was imperfect, in so far as some puncta were more red or green than yellow. This implies heterogeneity in glycosomal contents, which is discussed later. However, although the ratios of TbGAPDH (red) to NS enzyme (green) signals vary widely, quantitative analysis (Table 3) shows that the majority of the NS enzyme signals colocalize with punctate TbGAPDH signals, with the exception of TbPAGM.

Subcellular localization by digitonin latency

Digitonin latency is a powerful adjunct technique to assess whether soluble proteins are either cytosolic or sequestered in membrane-bound intracellular organelles. Digitonin is a steroidal-saponin detergent-like natural product that first permeabilizes and subsequently solubilizes biological membranes. Digitonin has a preference for high sterol content membranes. Thus, cytosolic soluble proteins are liberated from cells at very low digitonin concentrations, as the sterol-rich plasma membrane is the first affected, and organellar contents are subsequently liberated at significantly higher digitonin concentrations. The requirement for a higher digitonin concentration to effect protein release is known as 'digitonin latency'. This method has proved extremely useful in discriminating cytosolic versus glycosomal proteins in trypanosomatids, for example [42,58–60,61,69]. In our studies, we used the aforementioned mono-specific polyclonal mouse antibodies to eight nucleotide biosynthetic enzymes, along with rabbit antibodies to authentic glycosome lumen (TbGAPDH or TbAldolase), glycosome membrane (TbPEX13.1) and soluble cytosolic (TbEnolase) markers to assess digitonin latency of these enzymes in pcf and bsf trypanosomes (Fig 5A and 5B, respectively). As expected, the cytosolic marker, TbEnolase, was released from both lifecycle stages at very low digitonin concentrations whereas TbAldolase and TbGAPDH were not quantitatively released until 0.1% TX100 was used. This was not because the glycosome membrane was not being gradually solubilized by the digitonin, since the gradual release of membrane protein TbPEX13 was evident in these experiments, but because of the possibly aggregated nature of these very abundant proteins in what has been proposed to be a dense crystalloid core inside of glycosomes [56]. In contrast,

Anti-TbGNA	Anti-GAPDH	Merge	Phase
Anti-TbGNA	Anti-Enolase	Merge	Phase
Anti-TbPAGM	Anti-GAPDH	Merge	Phase
Anti-TbPAGM	Anti-Enolase	Merge	Phase
Anti-TbUAP	Anti-GAPDH	Merge	Phase
Anti-TbUAP	Anti-Enolase	Merge	Phase

10 µm

Fig 2. Immunofluorescence microscopy localisation of UDP-GlcNAc biosynthetic enzymes in procyclic form *T. brucei*. Enzymes of UDP-GlcNAc biosynthesis were localised with mono-specific mouse antibodies (green channels). Authentic glycosome and cytosol markers TbGAPDH and TbEnolase, respectively, were localised with specific rabbit antisera (red channels). Merged green and red channels and phase-contrast images are also shown.

TbPAGM showed a biphasic release pattern, consistent with dual cytoplasmic and glycosomal location. All the other nucleotide sugar biosynthetic enzymes showed release starting around 0.04 mg digitonin / mg protein, consistent with them being predominantly or exclusively glycosomal proteins. Interestingly, in all cases, the proteins seem to be slightly harder to release with digitonin from pcf cells than from bsf cells.

Subcellular localization by subcellular fractionation and evidence for glycosome heterogeneity by density gradient centrifugation and proteomics

Procyclic cells were lysed using a high-pressure homogenizer [54] and the lysate was subjected to differential centrifugation according to [70]. This procedure results in a nuclear fraction, a large granular fraction (LG), a small granular fraction (SG) and a cytoplasmic fraction (C), with the latter also containing microsomes of the plasma membrane, Golgi apparatus and endoplasmic reticulum (ER). These fractions were subjected to SDS-PAGE and Western blotting and the blots were probed with antibodies to authentic glycosomal, mitochondrial, cytoplasmic and ER markers (TbGAPDH, TbGAP1 [71], TbENO and calreticulin, respectively) which confirmed that the majority of mitochondrial TbGAP1 was in the LG fraction, that the majority of cytoplasmic TbENO and ER calreticulin was in the C fraction and that the majority of glycosomal TbGAPDH was in the SG fraction, as expected [70] (Fig 6A). Antibodies to three representative NS biosynthetic enzymes (TbPMI, TbMPGT and TbUGP) showed that these enzymes are found exclusively to the glycosome-containing SG fraction (Fig 6A, Table 1), consistent with the immunofluorescence microscopy and digitonin latency data described above.

The same SG fraction was further subjected to iodixanol density gradient centrifugation. Two opalescent bands (fractions 1 and 2) were observed (Fig 6B) at densities of 1.15 and 1.18 g/mL, similar to that reported for rat liver peroxisomes using iodixanol (1.175 g/mL) [72]. Each was isolated and, following reduction, alkylation and trypsin digestion of the protein content, subjected to proteomic analysis by liquid chromatography-tandem mass spectrometry (LC-MS/MS). The protein groups identified in both fractions were highly-enriched for glycosomal proteins, as expected. Intensity-based absolute quantitation (iBAQ) values were extracted for the protein groups belonging to a reference high-confidence glycosomal proteome [54]. These protein groups (x axis) are plotted against three iBAQ scales, from low abundance (iBAQ values $<1 \times 10^4$) to high-abundance (iBAQ values $>3 \times 10^6$), in (Fig 6C). Consistent with its higher density, fraction 2 contains more glycosomal protein than fraction 1. However, the relative abundances of glycsomal proteins between the two fractions are different, suggesting compositional heterogeneity between them.

Discussion

Evidence that NS biosynthetic enzymes might be glycosomal first came from the sequencing of the gene encoding TbGALE, the enzyme interconverts UDP-Glc and UDP-Gal. The predicted amino acid sequence contained a C-terminal peroxisomal targeting sequence type 1 (PTS1) of -TKL [41]. The glycosomal location of TbGALE was later confirmed experimentally in bsf and pcf cells [44]. A comprehensive screen of kinetoplastid genes for predicted PTS1 and N-terminal PTS2 sequences [65] added TbHK1 (PTS2), TbPGI (PTS1) and TbPMI (PTS1). TbUAP
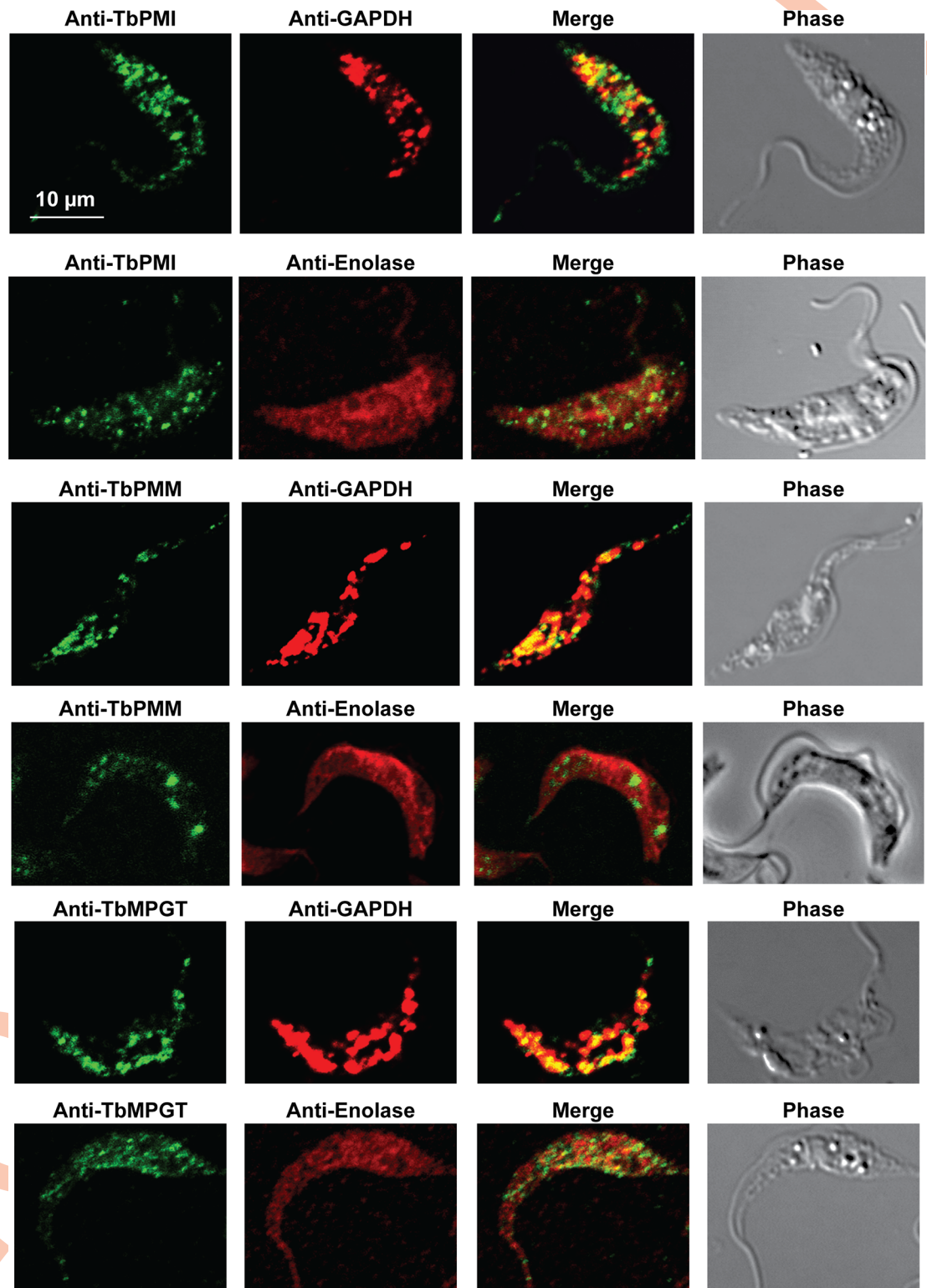
Fig 3. Immunofluorescence microscopy localisation of GDP-Man biosynthetic enzymes in procyclic form *T. brucei*. Enzymes of GDP-Man biosynthesis were localised with mono-specific mouse antibodies (green channels). Authentic glycosome and cytosol markers TbGAPDH and TbEnolase, respectively, were localised with specific rabbit antisera (red channels). Merged green and red channels and phase-contrast images are also shown.
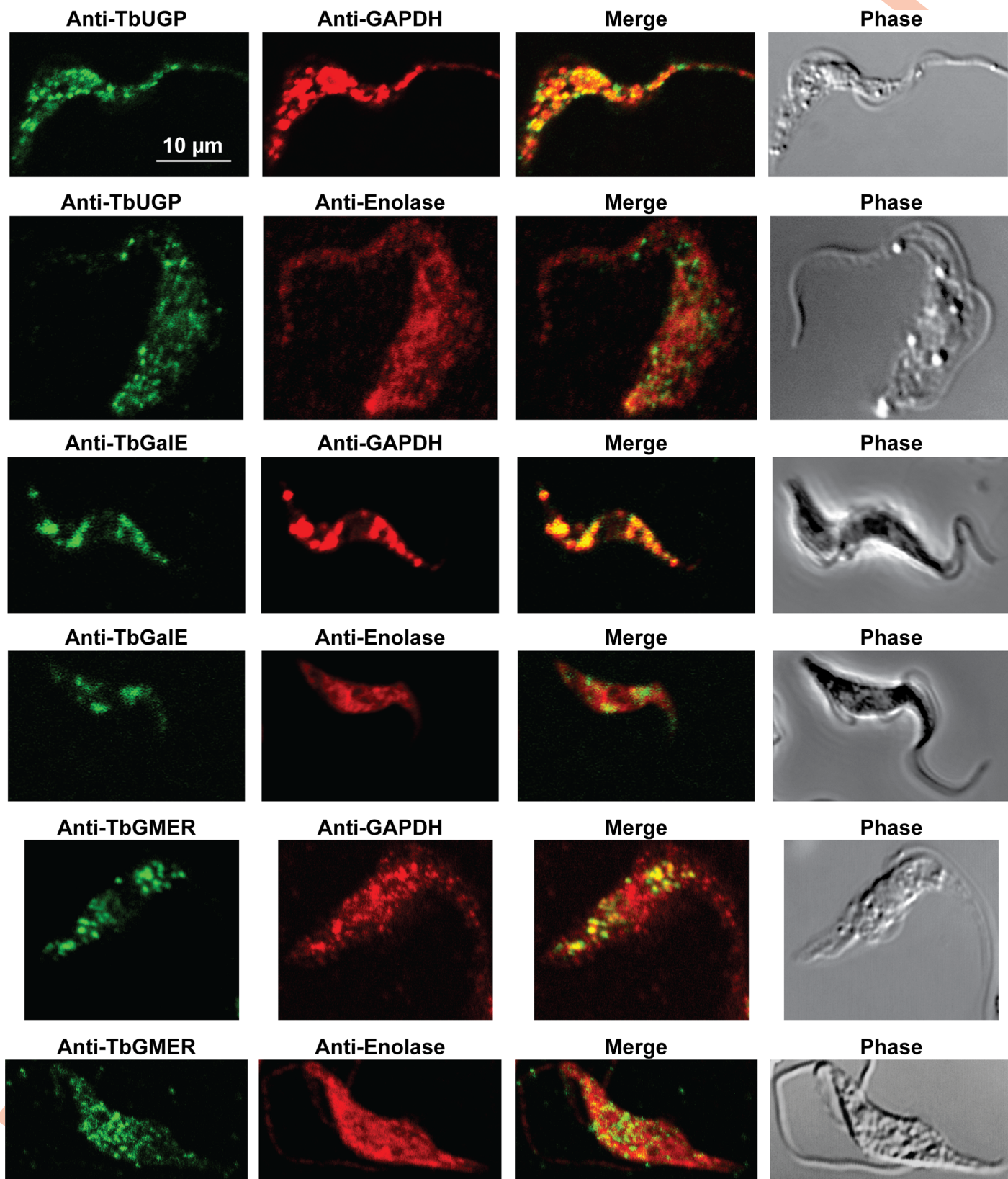
Fig 4. Immunofluorescence microscopy localisation of UDP-Glc, UDP-Gal and GDP-Fuc biosynthetic enzymes in procyclic form *T. brucei*. Enzymes of UDP-Glc, UDP-Gal and GDP-Fuc biosynthesis were localised with mono-specific mouse antibodies (green channels). Authentic glycosome and cytosol markers

TbGAPDH and TbEnolase, respectively, were localised with specific rabbit antisera (red channels). Merged green and red channels and phase-contrast images are also shown.

was later found to possess an atypical PTS1 sequence (-SNM) [50]. Interestingly, the HK1, GPI, UAP, and PMM enzymes of *T. cruzi* and *Leishmania major* also possess PTS motifs, as do the PMI and UGP enzymes of *T. cruzi* and *L. major*, respectively (Table 1). While many glycosomal components possess PTS signals for glycosomal import, many others do not. Internal targeting sequences have been proposed for *T. cruzi* phosphoglucomutase and *T. brucei* triose-phosphate isomerase [73,74] but these are not amenable to bioinformatic prediction. Other peroxisomal proteins are imported by a 'piggyback' mechanism through association with PTS-bearing proteins [75]. In this context, analysis of the protein complex database for pcf cells, using the cluster explorer function, suggests that TbPMM may piggyback on PTS1-containing TbPGI since both appear in cluster 314 in SEC300 gel-filtration and cluster 274 in SEC1000 gel-filtration [76]. The mapping of PTS1- and/or PTS2 -containing proteins to the high-confidence proteome for pcf glycosomes suggested a sensitivity and specificity of about 40% and 50%, respectively, for the bioinformatic prediction of glycosomal location [54]. Consequently, experimental confirmations of helpful PTS1/2 glycosomal location predictions are highly desirable.

Previously, the majority of immunofluorescence microscopy (IFM) localisation data for *T. brucei* NS biosynthetic enzymes were for bsf trypanosomes, with only TbGALE and TbGMD localised by IFM in pcf cells (Table 1). Now, all of the NS biosynthetic enzymes in pcf cells, except for TbPGI (that contains a PTS1 sequence and that is known to be glycosomal from sub-cellular fractionation) and for TbGFAT (which has proven difficult to express as a soluble protein for antibody production) have been successfully localised to the glycosome by IFM. The majority of these localisations, both for bsf and pcf cells, are further strongly supported here by digitonin latency experiments (Fig 5; Table 1). Further, subcellular fractionation and Western blotting for three representative NS biosynthetic enzymes (TbPMI, TbMPGT and TbUGP) show that these are found in the glycosome-containing small granular (SG) fraction (Fig 6A; Table 1).

Some of the IFM images (Figs 2, 3, and 4) show imperfect colocalization with the classical glycosomal marker in that the ratios of green NS enzyme- to red TbGAPDH-signals are variable. For example, some of the NS enzymes visually appear to occupy a subset of the

Table 3. Quantitative analysis of anti-NS enzyme and anti-TbGAPDH colocalization by IFM in pcf cells.

NS Enzyme	n[a]	Mander's colocalization coefficient[b]
TbGNA	6	0.85 ± 0.05
TbPAGM	5	0.33 ± 0.06
TbUAP	5	0.89 ± 0.02
TbPMI	9	0.96 ± 0.01
TbPMM	4	0.73 ± 0.06
TbMPGT	4	0.89 ± 0.04
TbUGP	8	0.89 ± 0.03
TbGalE	4	0.88 ± 0.05
TbGMER	7	0.88 ± 0.05

a n is number of cells uses in the analysis.

b The Mander's colocalization coefficient (± standard deviation of the mean) is a measure of the amount of green (anti-NS enzyme) signal above background that colocalizes with red (anti-TbGAPDH) stained compartments.
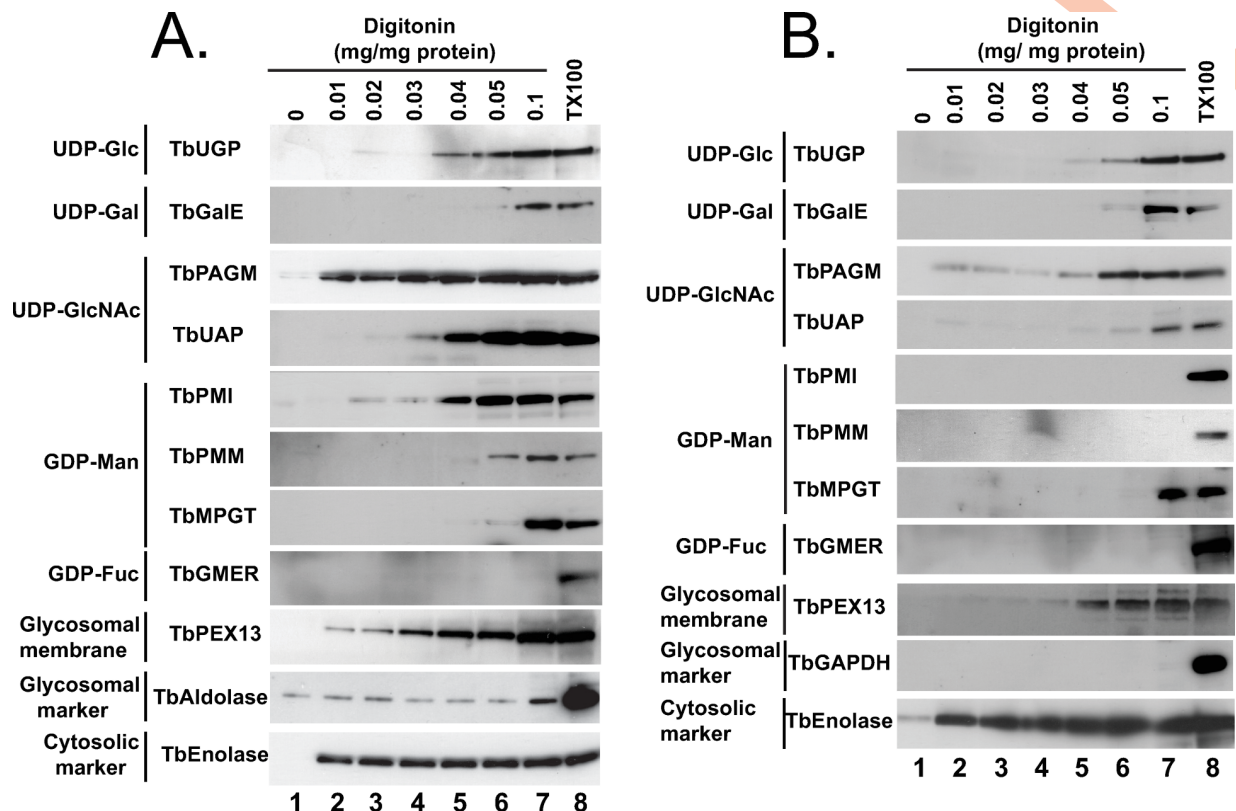
Fig 5. Digitonin latencies of nucleotide sugar biosynthetic enzymes in bloodstream and procyclic forms of *T. brucei*. Trypanosomes (bsf, panel A; pcf, panel B) were treated with increasing concentrations of digitonin (0.01 to 0.1 mg digitonin per mg trypanosome protein) and with no detergent and 0.1% TX100 as controls for no cell permeabilization and total cell and glycosome membrane permeabilization, respectively. The release of the cytoplasmic marker TbEnolase at the lowest digitonin concentration is consistent with the selective permeabilization of the plasma membrane over the glycosome membrane. The release of TbAldolase (panel A) or TbGAPDH (panel B) at higher digitonin concentrations, or only with 0.1% TX100, i.e., showing latency, is consistent with their known glycosome lumen locations. From the patterns of digitonin latency of the nucleotide sugar biosynthetic enzymes, we conclude that all shown, except TbPAGM, are principally or exclusively protected against release by digitonin by being sequestered in a low-sterol intracellular membrane-bound compartment.

TbGAPDH positive glycosomes (eg. for TbGNA, TbPMM, TbMPGT, TbUGP and TbGMER) whereas others show (green) glycosomes that contain less TbGAPDH (eg. for TbUAP, TbPMI, TbGALE). Similar results have been noted for bsf cells for TbPMM and TbPMI [42,46]. Nevertheless, quantitative analysis of the red and green channel signals across several cells (Table 3) shows that the majority of NS enzyme (green) signals colocalize with TbGAPDH (red) signals. Collectively, these data suggest some heterogeneity in glycosomal content, whereby the ratios of NS enzymes to TbGAPDH in individual glycosomes can vary quite widely. Whether this represents a mixture of immature and mature glycosomes or a mixture of different mature glycosomes, or a combination of both, is unclear from these data. However, glycosome biogenesis by growth and fission and by *de novo* biogenesis of nascent glycosomes that bud from the ER seems likely, as reviewed in [77]. Evidence for the latter can be found in our label-chase proteomic studies [54]. In this work, cells expressing GFP-tagged Pex13.1 were labelled to steady-state over 8 cell divisions with heavy isotope lysine and arginine and then placed into medium containing light lysine and arginine to perform a 5 h isotopic chase. Immediately after steady-state (heavy) labelling and after (light) chase, magnetic beads bearing anti-GFP antibodies were used to capture GFP-tagged Pex13.1 containing organelles which were taken for stable isotope in cell culture (SILAC) quantitative proteomics. At the steady-state label time point,
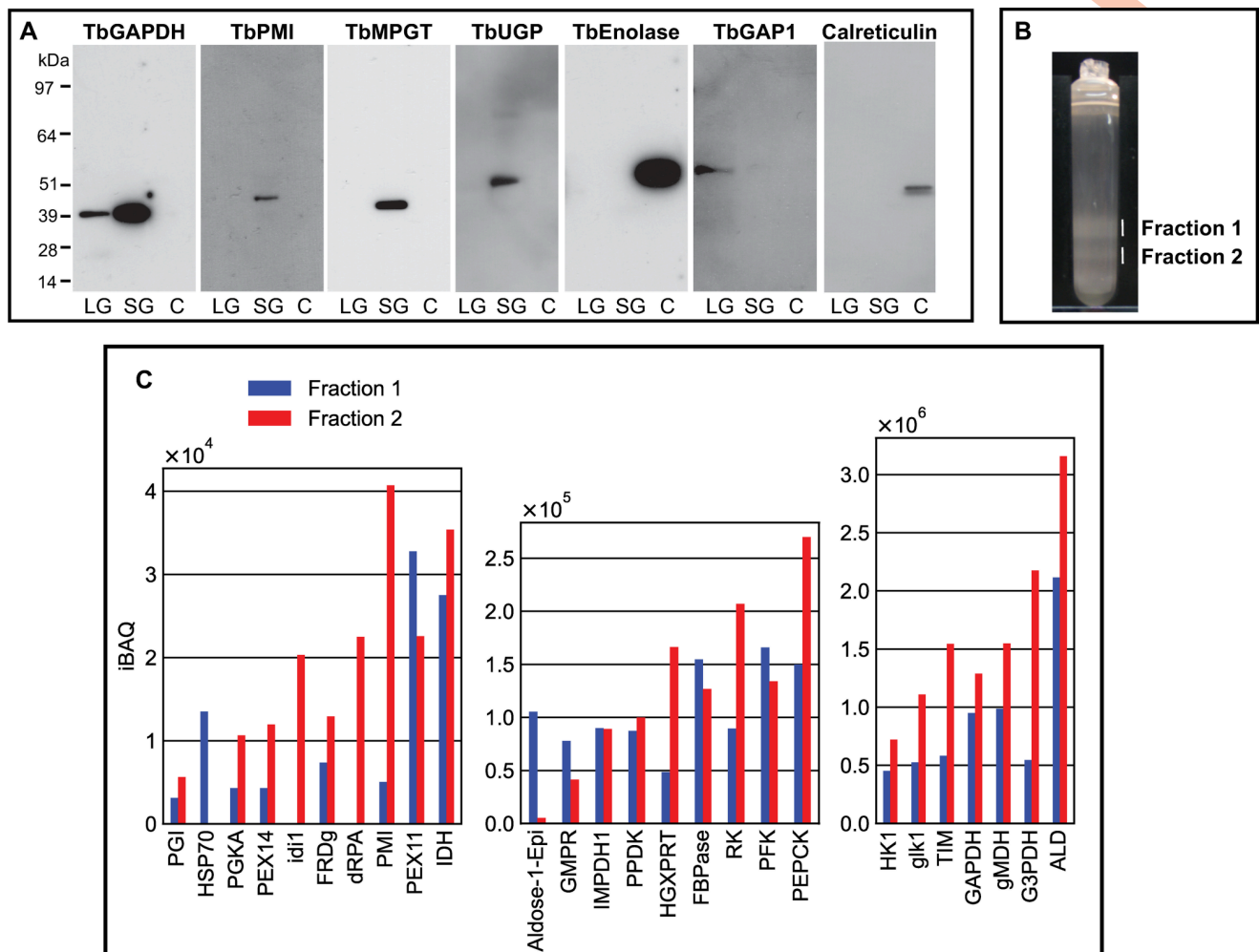
Fig 6. Subcellular localization by subcellular fractionation and evidence for glycosome heterogeneity by density gradient centrifugation and proteomics. Panel A: Pcf trypanosome lysate was submitted to differential centrifugation [70] and aliquots of the large granular (LG), small granular (SG) and cytosolic plus microsomal fractions (C) were subjected to SDS-PAGE and Western blotting with antibodies to authentic glycosomal (TbGAPDH), mitochondrial (TbGAP1), cytoplasmic (TbENO) and ER (calreticulin) markers and to NS biosynthetic enzymes (TbPMI, TbMPGT and TbUGP), as indicated. Panel B: The SG fraction was further fractionated by iodixanol density gradient centrifugation and two opalescent bands (fractions 1 and 2) were isolated. Panel 3: Aliquots of fractions 1 and 2 from panel B were subjected to proteomic analysis by LC-MS/MS. The relative abundances (iBAQ values over three scales, y-axes) are plotted against the identified proteins (TyiTrypDB identifiers, x-axes).

https://doi.org/10.1371/journal.pntd.0009132.g006

Pex13.1 was found associated with several ER resident proteins as well as glycosome components. However, after the light isotopic chase period, the apparent association of Pex13.1 with ER proteins was greatly diminished, suggesting that Pex13.1 and ER resident proteins part company during the biogenesis of glycosomes. Consistent with this, Bauer *et al.* showed by IFM and sub-cellular fractionation that Pex13.1 accumulates in the ER in pcf cells grown in low glucose [78]. The same group has also demonstrated the induction of glycosome heterogeneity in response to extracellular glucose levels [79], suggesting that the *de novo* and growth and division pathways of glycosome biogenesis are dynamic and responsive to changing environmental factors [77].

Also consistent with the aforementioned concept of glycosome heterogeneity, we found that we could resolve two glycosomal fractions by density gradient centrifugation (Fig 6B) and that the glycosomal protein contents of these two fractions were different (Fig 6C). In this

analysis, TbPMI was identified in both fractions but was enriched in fraction 2, consistent with the presence of TbPMI-rich (green and yellow) and TbPMI-poor (red) glycosomes in the TbPMI immunolocalization images (Fig 2B). Interestingly, proteins likely to be involved in protein import (glycosomal HSP70 and Pex11) are enriched in fraction 1, suggesting immature and actively importing glycosomes may be enriched in this lower density (lower protein content) fraction.

Only one of the NS biosynthetic enzymes (TbPAGM) appears to have dual location, being found in the cytoplasm as well as the glycosomes by IFM and digitonin latency (Fig 2, Table 3 and Fig 5). Whether TbPAGM has some role in cytoplasmic metabolism or whether this PTS-less protein is simply imported inefficiently into the glycosome remains to be determined.

Our localisation of TbMPGT, which converts Man1P to GDP-Man, to the glycosomes is at variance with a previous report using bsf cells that suggested a cytoplasmic location [48]. However, in that case the antibody used was raised to *L. major* MPGT and it is also possible that different growth conditions or other factors might account for this discrepancy. Several IFM localisations reported here do not agree well with those reported in the high-throughput TrypTag database [80]. In that case, eight epitope-tagged proteins, TbPGI, TbUGP, TbPAGM, TbUAP, TbPMI, TbPMM, TbGMD and TbGMER were variously described as flagellar cytoplasmic and/or nucleoplasmic and/or mitochondrial and/or cytoplasmic. However, C-terminal tagging of PTS1-containing TbPGI and TbPMI would likely cause their mislocalisation, and visual inspection of the IFM micrographs for N-terminally tagged TbUGP and TbPAGM suggests punctate staining reminiscent of glycosomes.

In summary, together with previously published sub-cellular fractionation data for TbHK1, TbPGI and TbGALE and glycosome proteome data for TbHK, TbPGI, TbUAP, TbGALE, TbUAP and TbPMI (Table 1), the data presented here provide a compelling case for the presence of the entire NS biosynthetic machinery in the glycosomes of both bsf and pcf *T. brucei*. This is radically different from other eukaryotes, where NS biosynthesis is either known or assumed to be located in the cytoplasm. The glycosomal location of NS biosynthesis in *T. brucei*, in turn, strengthens our postulate that an NS transporter (NST) or transporters is/are likely to exist in the bsf and pcf glycosome membranes to transport these large and negatively charged metabolites from the lumen of the glycosome into the cytoplasm. Once in the cytoplasm, NSs can be imported into the Golgi apparatus and ER by canonical SLC35-family NSTs [81] to perform glycosylation reactions in glycoprotein and glycolipid biosynthesis. The putative glycosomal NSTs may be quite different from the canonical SLC35-family NSTs since the direction of transport of the glycosomal NSTs (organelle lumen to cytosol) is in the opposite direction to that of the SLC35-family NSTs (cytosol to organelle lumen). It is possible that glycosomal NST(s) may provide a selective therapeutic target(s) for human and animal African trypanosomiasis.

Methods

Cell culture

Procyclic form *T. brucei* 427 strain containing T7 RNA polymerase and Tet repressor protein genes, respectively under control of G418 and hygromycin (clone 29.13.6 cells, kindly provided by George Cross) were grown at 28°C without CO_2 in original SDM-79 medium [82] containing hygromycin B (Roche) at 50 μg/ mL, G418 (Invitrogen) at 15 μg/ mL, 15% (v/v) heat inactivated fetal bovine serum (FBS), 2 g/L sodium bicarbonate, fresh 2 mM Glutamax I (Invitrogen) and 22.5 mg / ml haemin (added from a 0.05 M stock in NaOH), adjusted to pH 7.3. Bloodstream form *T. brucei* 427 strain containing T7 RNA polymerase and Tet repressor protein, under control of G418, known as single markers cells, kindly provided by George

Cross, were grown at 37˚C with 5% CO_2 in HMI-9T medium [83] containing fresh 2mM Glutamax I (Invitrogen) and 2.5 μg/ mL G418 (Invitrogen).

Production of recombinant TbMPGT

The TbMPGT ORF (gene Tb927.8.2050) was amplified from genomic DNA by PCR and cloned into pET28a, containing a 6-His N-terminal tag with a thrombin cleavage site, and overexpressed in BL21 (DE 3) Gold *E. coli* grown at 37˚C in LB medium supplemented with kanamycin (50 μg / ml) and tetracycline (10 μg / ml). When the OD_{600} reached about 2.0, the temperature was lowered to 16˚C and protein expression was induced with 1 mM IPTG (Formedium) for 22 h. Cells were harvested, resuspended in lysis buffer (20 mM Tris, 500 mM NaCl, 20 mM imidazole, pH 8.0), supplemented with DNAse I and EDTA-free protease inhibitors (Roche), disrupted using a French press and centrifuged at 30,000 g for 30 min at 4˚. The supernatant was filtered (0.2 μm) and applied to a 5 ml HisTrap HP chelating column (GE healthcare), pre-equilibrated in lysis buffer, and eluted with a linear imidazole gradient from 96% buffer A (20 mM Tris, 500 mM NaCl, pH 8) to 100% buffer B (20 mM Tris, 500 mM NaCl, 500 mM imidazole, pH 8). Fractions containing TbMPGT (which eluted around 300 mM imidazole) were pooled, concentrated, digested with thrombin (NEB) to remove the His-tag and subsequently purified on a Superose 12 10/300 column (GE healthcare) equilibrated with 10 mM Hepes, 100mM NaCl, pH 7.4. The yield, estimated by BCA assay, was about 10 mg of soluble, enzymatically active and highly purified TbMPGT per litre of culture (S1 Fig). The identity of the recombinant TbMPGT was confirmed by proteomics.

Production of mouse antibodies against recombinant nucleotide sugar biosynthetic enzymes

Aliquots of recombinant purified TbMPGT (S1 Fig), TbGALE [41], TbGNA [49], TbUAP [50] and TbGMER [52] were submitted to David's Biotech (Germany) for the immunization of two mice per protein, according to their recommended protocol using Freund's complete adjuvant for the primary immunisation with 0.1 mg protein per mouse and two secondary boosts with 0.05 mg per mouse in Freund's incomplete adjuvant. Pooled mouse anti-TbMPGT, anti-TbUAP and anti-TbGNA sera were immunopurified by affinity chromatography on Sepharose4B beads coupled to recombinant TbMPGT, TbUAP and TbGNA, respectively, at 3–5 mg / ml gel. The affinity chromatography beads were prepared using CNBr-Sepharose 4B (GE Healthcare) according to the manufacturer's instructions. The coupled beads were stored in phosphate buffered saline (PBS) containing 0.05% (w/v) sodium azide. For affinity purification, pooled mouse sera were centrifuged at 16,000 g for 15 min at 4˚C and the supernatants mixed with an equal volume of PBS. These were incubated with the corresponding affinity chromatography beads for 2 h with rotation at 4˚C. The beads were washed with PBS until the optical density at 280 nm (OD280) of the supernatant was below 0.05 and the specifically bound antibodies were then eluted with 50 mM sodium citrate pH 2.8. The eluates were immediately neutralized with 1M Tris-HCl pH 8.8 and quantitated by OD280.

Immunoprecipitation

T. brucei bsf cells were washed three times with trypanosome dilution buffer (TBD; 20 mM Na_2HPO_4, 2 mM NaH_2PO_4, 80 mM NaCl, 5 mM KCl, 1 mM $MgSO_4$, 20 mM glucose pH 7.7) and lysed at 1×10^9 cells/ml in 1% (w/v) SDS in 20 mM Tris-HCl pH 6.8 containing 0.1 M DTT and heated at 50˚C for 15 min. The SDS lysate was diluted to 0.03% SDS with 1% (w/v) Triton X-100 in 20 mM Tris-HCl pH 6.8, 0.15 M NaCl, 0.1 mM TLCK, 1 μg / ml leupeptin, 1 μg / ml aprotinin and 1 mM PMSF. Insoluble material was removed by centrifugation at

16,000 g for 10 min at 4˚C and an aliquot of the supernatant (equivalent to 2 x 10^8 cells) was incubated with 5 µL of rabbit anti-TbGalE antiserum [44] for 1 h at 4˚C and immunoprecipitated with 50µL of Protein A magnetic beads (Invitrogen). A similar procedure was used for TbGMER immunoprecipitation, but instead mouse antisera anti-GMER and protein G magnetic beads (Invitrogen) were used. Samples were run in SDS-PAGE for Western blotting.

Western blotting

Samples were run on 4–12% gradient NuPAGE gels (Invitrogen) and Western blotted onto nitrocellulose using an iBlot system (Invitrogen). The pieces of nitrocellulose were either stained with Ponceau red for protein or blocked with 30 ml pre-filtered (20 µm) blocking buffer (50 mM Tris-HCl pH 7.4 containing 0.15 M NaCl, 0.25% BSA (w/v), 2% (w/v) fish skin gelatin and 0.05% (w/v) Tween 20) using a SNAPid system (Millipore). The latter were incubated with 0.5–1 µg / ml affinity purified antibody or with 1:1,000 diluted mouse antiserum (both diluted in blocking buffer) against the respective nucleotide sugar biosynthetic enzymes for 1 h at room temperature. Using the SNAPid system, the blots were washed 3 times 30 ml PBS, 0.1% Tween 20 and then incubated with 5 ml anti-mouse HRP (Invitrogen) diluted 1:10,000 in blocking buffer without sodium azide. The blots were subsequently washed with PBS, 0.1% Tween 20, removed from the SNAPid system and developed with ECL (Thermo-Fisher). Rabbit anti-TbGAPDH, rabbit anti-TbEnolase, rabbit anti-TbPEX13 and rabbit anti-TbAldolase (kind gifts from Prof. Paul Michels, Univ. of Edinburgh, UK) were used at 1:5,000, 1:5,000, 1:10,000 and 1:5,000 dilutions in blocking buffer, respectively. In addition, developments with mitochondrial marker [rabbit anti-TbGAP1 (a kind gift from Prof. Julius Luke, Institute of Parasitology, Czech Republic)] were performed at a dilution of 1:1,500 and developments with ER marker [immunopurified rabbit anti-calreticulin (Stressgen, Enzo LifeSci, USA)] were performed at a dilution of 1:1,000. Blots were developed with 1:10,000 anti-rabbit HRP (Invitrogen) and ECL reagents according to the manufacturer's instructions (Thermo-Fisher). The blots were exposed onto ECL film (GE Healthcare Amersham), developed and scanned in an Epson office scanner.

Immunofluorescence microscopy

Trypanosomes were washed in ice-cold phosphate buffer saline (PBS) for pcf cells or ice-cold trypanosome dilution buffer (TDB; 20 mM Na_2HPO_4, 2 mM NaH_2PO_4, 80 mM NaCl, 5 mM KCl, 1 mM $MgSO_4$, 20 mM glucose, pH 7.7) for bsf cells and resuspended in the same buffer. Equal volumes of 8% paraformaldehyde (PFA) in PBS or TDB, respectively, were added and cells were fixed at 4˚ C. Subsequently, suspensions of fixed cells were spotted on cover slips, allowed to air dry, permeablized with 0.1% TX100 in PBS for 10 min and blocked in PBS, 5% fish skin gelatin, 10% normal goat serum and 0.05% TX100. Affinity purified anti-TbMPGT, anti-TbUGP and anti-TbGNA mouse antibodies were used at 0.5–1.0 µg / ml diluted in PBS, 1% fish skin gelatin, 0.05% TX100 and incubated for 1 h at room temperature in a humid chamber. Anti-TbGALE, anti-TbPAGM, anti-TbPMI, anti-TbPMM and anti-TbGMER mouse sera were diluted at 1:500 or 1:1,000 in the same buffer. Rabbit anti-GAPDH and rabbit anti-TbEnolase sera (generous gifts of Dr Paul Michels) were used at 1:2,000 and 1:4,000 dilution, respectively. Coverslips were washed in PBS, 1% fish skin gelatin, 0.05% TX100 and incubated for 1 h at room temperature with 50 µL goat anti-mouse IgG Alexa 488 conjugated mixed goat anti-rabbit IgG Alexa 594 conjugated, both diluted at 1:500 in same buffer. Coverslips were washed and mounted on glass slides using Prolong Gold (Invitrogen). Microscopic images were obtained in a Zeiss LSM 710 META confocal microscope.

Colocalisations were quantified using Volocity software (Quorum Technologies). Zeiss.lsm images were imported into the Volocity library and processed as follows: The thresholds for the red and green channels were calculated from a region of interest outside the cell images. Individual cells were selected using the region of interest (ROI) tool and colocalization statistics were calculated and recorded for each cell. Mander's colocalisation coefficients (the fraction of green signal colocalising with red compartments) are reported in (Table 3), according to the recommendations of [84].

Digitonin latency

Digitonin latency was performed as previously described in [42]. Briefly *T.brucei* bloodstream or procyclic form cells (2 x 10^9 cells) were washed twice with 10 ml 250 mM sucrose, 25 mM Tris-HCl pH 7.4 and 1 mM EDTA (STE buffer) and resuspended in 1.5 ml STEN (STE containing 0.15 M NaCl). Aliquots (0.15 ml) were treated with equal volume of digitonin at various concentrations in the presence of 0.1 mM TLCK, 1 μg / ml leupeptin, 1 μg / ml aprotinin and 1 mM PMSF. Digitonin stock was prepared at 10 mg / ml in DMSO and diluted in STEN to the required concentrations. Complete extraction was obtained in parallel by treating an equivalent number of cells with 0.1% Triton X-100 in STEN. The lysates were incubated for 5 min at room temperature and the insoluble materials removed by centrifugation at 16,000 g for 2 min. The pellets were discarded and samples of the supernatants were run on a reducing 4–12% gradient NuPage gel (Invitrogen) and transferred to nitrocellulose for Western blotting using antisera produced in mouse and at the dilutions described in the immunofluorescence section. Different amounts of same samples were loaded onto separate gels for each antibody Western blot, in order to keep within the linear range of film exposure. For *Tb*PMM, TbGALE and TbGMER 1x10^7 cell equivalents per lane, for TbPAGM, TbMPGT, TbUGP, TbUAP, TbPMI, 5 x 10^6 cell equivalents per lane, for TbGAPDH, TbAldolase (Aldo), for TbEnolase (Eno) 1x10^5 cell equivalents per lane and for TbPEX13 5x10^6 cell equivalents per lane.

Subcellular fractionation by differential centrifugation followed by density gradient centrifugation

The pcf cells used for differential and density gradient centrifugation came from a stable isotope in cell culture (SILAC) labelling experiment. However, the isotopic labelling is not relevant to the specific experiments and results presented here. The starting pcf cell preparation (a total of 5.6 x 10^9 cells washed in STE buffer) was a 1: 1 mixture of (i) GFP-tagged PEX13.1 pcf mutants labelled to steady state over 8 cell divisions, and to a final cell density of 1.1.x 10^7 cells / ml, in R6K6 SDM-79 medium containing heavy isotopes of L-Arginine (R6) and L-Lysine (K6), and (ii) double marker cells grown in normal SDM-79 medium (R0K0) and also harvested at 1.1 x 10^7 cells / ml.

The mixed cells were lysed using a One-shot high-pressure cell disruptor (Constant Systems, UK) operated at 10,000 psi as described in [54]. The lysate was submitted to differential centrifugation as described in [70]: After spinning at 1,500 g to the remove nuclei and any remaining intact cells and cell ghosts, the supernatant was submitted to centrifugation at 5,000 g to yield a Large Granular fraction (LG) pellet, enriched in mitochondria. Subsequent centrifugation of the supernatant at 15,000 g pelleted the Small Granular fraction (SG), enriched in glycosomes, with concomitant generation of a supernatant (C) enriched in cytosol and ER, Golgi and plasma membrane microsomes.

The SG fraction was subsequently submitted to density gradient centrifugation using iodixanol (Optiprep, Axis Shield, UK) according to [53], with some modifications: A discontinuous step gradient of iodixanol was prepared by layering 20, 25, 30, 35, 40 and 45% (w/v) iodixanol

in STE buffer inside an Optiseal polyallomer tube (Beckman) using a peristaltic pump to apply each layer to the bottom of the tube, starting with the least dense layer and displacing it with next dense layer and so on. The SG fraction resuspended in STE buffer was loaded carefully on top of the gradient and centrifuged at 45,000 rpm using VTi-50 vertical rotor in a Beckman ultracentrifuge for 1h at 4˚C. After ultracentrifugation, the tube was punctured with needle and syringe to collect 2 distinct opalescent bands, fraction 1 (top band) and fraction 2 (lower band). The refractive index of each fraction was measured using a refractometer (Abbe refractometer model NAR-1T) and plotted against a standard curve of 20, 25, 30, 35, 40 and 45% (w/v) iodixanol in STE. The density was calculated according to published tables of iodixanol percentage versus density (g/mL).

Proteomic analyses

Samples of fraction 1 and fraction 2 were reduced with dithiothreitol and alkylated with iodoacetamide and subsequently digested with trypsin and processed using FASP II (filter-aided sample processing), as described previously in [54]. Samples were desalted using a custom made Porous R2 columns packed with 1.5 mg Porous R2 reverse phase beads (ABI). The columns were pre-conditioned by washing with 90% CH_3CN containing 0.1% formic acid followed by equilibration in 0.1% formic acid in water. Samples were applied in 0.1% formic acid and the columns washed with 0.1% formic acid then subsequently eluted three times with 90% CH_3CN containing 0.1% formic acid. The eluates were combined, dried in a Speedvac vacuum concentrator, resuspended in 35% CH_3CN containing 0.1% formic acid and fractionated using strong cation exchange (SCX) chromatography: The combined eluates were applied into a custom made SCX column made by adding Poros 50 HS SCX beads (ABI) to a SCX Ziptip (Millipore). Bound peptides were eluted sequentially with 20, 100, 150, and 200 mM NaCl in 35% CH_3CN containing 0.1% formic acid, followed by final elutions with 0.5% NH_4OH in 50% isopropanol and 50% isopropanol (IPA sample). Each of these five sub-fractions were dried and re-suspended in 50 μL 1% formic acid and 15 μL aliquots were subjected to liquid chromatography on Ultimate 3000 RSLCnano system (Thermo Scientific) fitted with an Acclaim PepMap 100 (C18, 100 μM x 2 cm) trap cartridge. Peptides were separated on an Easy-Spray PepMap RSLC C18 column (75 μM x 50 cm) (Thermo Scientific) using a linear gradient from 2 to 40% buffer B (80% acetonitrile, 0.1% formic acid) in buffer A (0.1% formic acid) over 70 min. The HPLC system was coupled to a Orbitrap Velos Mass Spectrometer (Thermo Scientific) with a source voltage of 1.2 kV.

Proteomic data analysis

LC-MS/MS data were analysed for protein identification using MaxQuant 1.6.14 [85,86] with the in-built Andromeda search engine [87]. The raw files were searched against the *T. brucei brucei* 927 annotated protein sequences from TriTrypDB release 46 [88] supplemented with the *T. brucei brucei* 427 VSG221 (Tb427.*BES40.22*) protein sequence. The mass tolerance was set to 4.5 ppm for precursor ions and trypsin was set as proteolytic enzyme with two missed cleavage allowed. Carbamidomethyl on cysteine was set as fixed modifications. SILAC labelling [5] of heavy arginine (Arg-6) and Lysine (Lys-6) were specified. Oxidation of methionine and Acetylation of Protein N-term were set as variable modifications. The false-discovery rate for protein and peptide level identifications was set at 1%, using a target-decoy based strategy. The minimum peptide length was set to seven amino acids and protein quantification was performed on unique plus razor peptides [89]. "Reverse Hits", "Only identified by site" and "Potential contaminant" identifications were filtered out. Only protein groups with at least two unique peptide sequences and Andromeda protein score greater than 5 were selected for

further analysis. The high confidence glycosomal resident proteins were extracted from Güther *et al.*, 2014 [54]. Gene abbreviations were retrieved from the TriTrypDB database. The iBAQ values [89,90] were extracted from the MaxQuant output and visualised as bar graphs. The analysis pipeline was implemented in python using the SciPy packages (https://www.scipy.org/) and Jupyter notebook (https://jupyter.org/).

The mass spectrometry proteomics data have been deposited to the ProteomeXchange Consortium via the PRIDE [91] partner repository with the dataset identifier PXD023124. Reviewer account details: **Username:** reviewer_pxd023124@ebi.ac.uk. **Password:** qqm7vZg3. The analysis pipeline is available in GitHub (https://github.com/mtinti/nucleotide_sugar) and it is archived in Zenodo (https://doi.org/10.5281/zenodo.4289929). The analysis pipeline is reproducible using the mybinder app with the link reported in the GitHub repository.

Supporting information

S1 Fig. Recombinant TbMPGT. Analysis by SDS-PAGE and Coomassie blue staining of TbMPGT expressed in *E.coli*, purified by nickel chromatography, digested with thrombin to remove the N-terminal 6-His tag and then purified by FPLC gel-filtration. Molecular weight standards are shown on the left.
(DOCX)

S2 Fig. Mono-specificity of antibodies to nucleotide sugar biosynthetic enzymes used in this study. The mouse polyclonal antibodies raised against TbMPGT, TbGNA, TbUAP, TbGALE and TbGMER (Tables 1 and 2) were used in Western blotting with an anti-mouse-HRP secondary antibody. The lanes contained either 5×10^6 cell equivalents of *T. brucei* bsf total cell lysates (lanes 1, 2, 3, 5, and 7) or, when no signal was recorded against whole lysate due to low abundance, the lanes contained an immunoprecipitate from 2×10^8 cell equivalents of total bsf lysate using rabbit anti-TbGALE [44] (lane 4) or mouse anti-TbGMER (lane 6). In each case, a single band* with an apparent molecular weight consistent with the target antigen was recorded, demonstrating the mono-specificity of the antibodies. *Note: the two additional bands marked by asterixis in (lane 6) are due to mouse IgG heavy and light chains from the immunoprecipitation. A Ponceau red stain of a Western blot lane containing 5×10^6 cell equivalents of *T. brucei* bsf total cell lysate is shown in (lane 8). The positions of MW standards are shown on the right.
(DOCX)

Acknowledgments

Author Contributions

Conceptualization: Maria Lucia Sampaio Guther, Michael A. J. Ferguson.

Data curation: Maria Lucia Sampaio Guther, Alan R. Prescott, Michele Tinti.

Formal analysis: Maria Lucia Sampaio Guther, Alan R. Prescott, Michele Tinti, Michael A. J. Ferguson.

Funding acquisition: Michael A. J. Ferguson.

Investigation: Maria Lucia Sampaio Guther, Alan R. Prescott.

Methodology: Maria Lucia Sampaio Guther, Alan R. Prescott, Sabine Kuettel.

Project administration: Maria Lucia Sampaio Guther, Michael A. J. Ferguson.

Resources: Maria Lucia Sampaio Guther, Alan R. Prescott, Sabine Kuettel, Michele Tinti.

Software: Alan R. Prescott, Michele Tinti.

Supervision: Maria Lucia Sampaio Guther, Michael A. J. Ferguson.

Validation: Maria Lucia Sampaio Guther, Alan R. Prescott, Michele Tinti.

Visualization: Maria Lucia Sampaio Guther, Alan R. Prescott, Michele Tinti.

Writing – original draft: Maria Lucia Sampaio Guther, Alan R. Prescott, Michele Tinti, Michael A. J. Ferguson.

Writing – review & editing: Maria Lucia Sampaio Guther, Michael A. J. Ferguson.

References

1. Schwede A, Macleod OJS, MacGregor P, Carrington M. (2015) How Does the VSG Coat of Blood-stream Form African Trypanosomes Interact with External Proteins? PLoS Pathog 11, e1005259 https://doi.org/10.1371/journal.ppat.1005259 PMID: 26719972

2. Salmon D., Geuskens M., Hanocq F., Hanocq-Quertier J., Nolan D., Ruben L., and Pays E. (1994) A novel heterodimeric transferrin receptor encoded by a pair of VSG expression site-associated genes in T. brucei. Cell 78, 75–86 https://doi.org/10.1016/0092-8674(94)90574-6 PMID: 8033214

3. Trevor CE, Gonzalez-Munoz AL, Macleod OJS, Woodcock PG, Rust S, Vaughan TJ, et al. Structure of the trypanosome transferrin receptor reveals mechanisms of ligand recognition and immune evasion. Nat Microbiol. 2019; 4(12):2074–81. https://doi.org/10.1038/s41564-019-0589-0 PMID: 31636418

4. Mehlert A., Wormald M. R., and Ferguson M. A. J. (2012) Modeling of the N-glycosylated transferrin receptor suggests how transferrin binding can occur within the surface coat of Trypanosoma brucei. PLoS Pathog 8, e1002618 https://doi.org/10.1371/journal.ppat.1002618 PMID: 22496646

5. Peck R. F., Shiflett A. M., Schwartz K. J., McCann A., Hajduk S. L., and Bangs J. D. (2008) The LAMP-like protein p67 plays an essential role in the lysosome of African trypanosomes. Mol Microbiol 68, 933–946 https://doi.org/10.1111/j.1365-2958.2008.06195.x PMID: 18430083

6. Jackson A. P., Allison H. C., Barry J. D., Field M. C., Hertz-Fowler C., and Berriman M. (2013) A cell-surface phylome for African trypanosomes. PLoS Negl Trop Dis 7, e2121 https://doi.org/10.1371/journal.pntd.0002121 PMID: 23556014

7. Allison H., O'Reilly A. J., Sternberg J., and Field M. C. (2014) An extensive endoplasmic reticulum-localised glycoprotein family in trypanosomatids. Microb Cell 1, 325–345 https://doi.org/10.15698/mic2014.10.170 PMID: 26167471

8. Lingnau A., Zufferey R., Lingnau M., and Russell D. G. (1999) Characterization of tGLP-1, a Golgi and lysosome-associated, transmembrane glycoprotein of African trypanosomes. J Cell Sci 112 Pt 18, 3061–3070 PMID: 10462522

9. Engstler M., Weise F., Bopp K., Grunfelder C. G., Gunzel M., Heddergott N., and Overath P. (2005) The membrane-bound histidine acid phosphatase TbMBAP1 is essential for endocytosis and membrane recycling in Trypanosoma brucei. J Cell Sci 118, 2105–2118 https://doi.org/10.1242/jcs.02327 PMID: 15855239

10. LaCount D. J., Barrett B., and Donelson J. E. (2002) Trypanosoma brucei FLA1 is required for flagellum attachment and cytokinesis. J Biol Chem 277, 17580–17588 https://doi.org/10.1074/jbc.M200873200 PMID: 11877446

11. Woods K, Nic a'Bhaird N, Dooley C, Perez-Morga D, Nolan DP. Identification and characterization of a stage specific membrane protein involved in flagellar attachment in Trypanosoma brucei. PLoS One. 2013; 8(1):e52846. https://doi.org/10.1371/journal.pone.0052846 PMID: 23335957

12. Higgins MK, Tkachenko O, Brown A, Reed J, Raper J, Carrington M. Structure of the trypanosome haptoglobin-hemoglobin receptor and implications for nutrient uptake and innate immunity. Proc Natl Acad Sci U S A. 2013; 110(5):1905–10. https://doi.org/10.1073/pnas.1214943110 PMID: 23319650

13. Zoll S, Lane-Serff H, Mehmood S, Schneider J, Robinson CV, Carrington M, et al. The structure of serum resistance-associated protein and its implications for human African trypanosomiasis. Nat Microbiol. 2018; 3(3):295–301. https://doi.org/10.1038/s41564-017-0085-3 PMID: 29358741

14. Macleod OJS, Bart JM, MacGregor P, Peacock L, Savill NJ, Hester S, et al. A receptor for the complement regulator factor H increases transmission of trypanosomes to tsetse flies. Nat Commun. 2020; 11 (1):1326. https://doi.org/10.1038/s41467-020-15125-y PMID: 32165615

15. Casas-Sánchez A, Perally S, Ramaswamy R, Haines LR, Rose C, Yunta C, et al. bioRxiv 477737; https://doi.org/10.1101/477737

16. Treumann A., Zitzmann N., Hulsmeier A., Prescott A. R., Almond A., Sheehan J., and Ferguson M. A. (1997) Structural characterisation of two forms of procyclic acidic repetitive protein expressed by procyclic forms of Trypanosoma brucei. J Mol Biol 269, 529–547 https://doi.org/10.1006/jmbi.1997.1066 PMID: 9217258

17. Acosta-Serrano A., Cole R. N., Mehlert A., Lee M. G., Ferguson M. A., and Englund P. T. (1999) The procyclin repertoire of Trypanosoma brucei. Identification and structural characterization of the Glu-Pro-rich polypeptides. J Biol Chem 274, 29763–29771 https://doi.org/10.1074/jbc.274.42.29763 PMID: 10514452

18. Guther M. L., Lee S., Tetley L., Acosta-Serrano A., and Ferguson M. A. (2006) GPI-anchored proteins and free GPI glycolipids of procyclic form Trypanosoma brucei are nonessential for growth, are required for colonization of the tsetse fly, and are not the only components of the surface coat. Mol Biol Cell 17, 5265–5274 https://doi.org/10.1091/mbc.e06-08-0702 PMID: 17035628

19. Guther M. L., Beattie K., Lamont D. J., James J., Prescott A. R., and Ferguson M. A. (2009) Fate of glycosylphosphatidylinositol (GPI)-less procyclin and characterization of sialylated non-GPI-anchored surface coat molecules of procyclic-form Trypanosoma brucei. Eukaryot Cell 8, 1407–1417 https://doi.org/10.1128/EC.00178-09 PMID: 19633269

20. Zamze S. E., Wooten E. W., Ashford D. A., Ferguson M. A., Dwek R. A., and Rademacher T. W. (1990) Characterisation of the asparagine-linked oligosaccharides from Trypanosoma brucei type-I variant surface glycoproteins. Eur J Biochem 187, 657–663 https://doi.org/10.1111/j.1432-1033.1990.tb15350.x PMID: 2303059

21. Zamze S. E., Ashford D. A., Wooten E. W., Rademacher T. W., and Dwek R. A. (1991) Structural characterization of the asparagine-linked oligosaccharides from Trypanosoma brucei type II and type III variant surface glycoproteins. J Biol Chem 266, 20244–20261 PMID: 1939085

22. Atrih A., Richardson J. M., Prescott A. R., and Ferguson M. A. J. (2005) Trypanosoma brucei glycoproteins contain novel giant poly-N-acetyllactosamine carbohydrate chains. J Biol Chem 280, 865–871 https://doi.org/10.1074/jbc.M411061200 PMID: 15509560

23. Izquierdo L., Atrih A., Rodrigues J. A., Jones D. C., and Ferguson M. A. J. (2009) Trypanosoma brucei UDP-glucose:glycoprotein glucosyltransferase has unusual substrate specificity and protects the parasite from stress. Eukaryotic cell 8, 230–240 https://doi.org/10.1128/EC.00361-08 PMID: 19114500

24. Acosta-Serrano A., O'Rear J., Quellhorst G., Lee S. H., Hwa K. Y., Krag S. S., and Englund P. T. (2004) Defects in the N-linked oligosaccharide biosynthetic pathway in a Trypanosoma brucei glycosylation mutant. Eukaryot Cell 3, 255–263 https://doi.org/10.1128/ec.3.2.255-263.2004 PMID: 15075256

25. Ferguson M. A., Homans S. W., Dwek R. A., and Rademacher T. W. (1988) Glycosyl-phosphatidylinositol moiety that anchors Trypanosoma brucei variant surface glycoprotein to the membrane. Science 239, 753–759 https://doi.org/10.1126/science.3340856 PMID: 3340856

26. Guther M. L., and Ferguson M. A. (1993) The microanalysis of glycosyl-phosphatidylinositol glycans. Methods Mol Biol 14, 99–117 https://doi.org/10.1385/0-89603-226-4:99 PMID: 8348247

27. Mehlert A., Richardson J. M., and Ferguson M. A. (1998) Structure of the glycosylphosphatidylinositol membrane anchor glycan of a class-2 variant surface glycoprotein from Trypanosoma brucei. J Mol Biol 277, 379–392 https://doi.org/10.1006/jmbi.1997.1600 PMID: 9514751

28. Mehlert A., Sullivan L., and Ferguson M. A. (2010) Glycotyping of Trypanosoma brucei variant surface glycoprotein MITat1.8. Mol Biochem Parasitol 174, 74–77 https://doi.org/10.1016/j.molbiopara.2010.06.007 PMID: 20558211

29. Mehlert A., and Ferguson M. A. (2007) Structure of the glycosylphosphatidylinositol anchor of the Trypanosoma brucei transferrin receptor. Mol Biochem Parasitol 151, 220–223 https://doi.org/10.1016/j.molbiopara.2006.11.001 PMID: 17140675

30. Izquierdo L., Nakanishi M., Mehlert A., Machray G., Barton G. J., and Ferguson M. A. (2009) Identification of a glycosylphosphatidylinositol anchor-modifying beta1-3 N-acetylglucosaminyl transferase in Trypanosoma brucei. Mol Microbiol 71, 478–491 https://doi.org/10.1111/j.1365-2958.2008.06542.x PMID: 19040631

31. Ferguson M. A. J., Hart G. W., and Kinoshita T. (2015) Glycosylphosphatidylinositol Anchors. in Essentials of Glycobiology (rd, Varki A., Cummings R. D., Esko J. D., Stanley P., Hart G. W., Aebi M., Darvill

A. G., Kinoshita T., Packer N. H., Prestegard J. H., Schnaar R. L., and Seeberger P. H. eds.), Cold Spring Harbor (NY). pp 137–150

32. Pinger J, Nesic D, Ali L, Aresta-Branco F, Lilic M, Chowdhury S, et al. African trypanosomes evade immune clearance by O-glycosylation of the VSG surface coat. Nat Microbiol. 2018; 3(8):932–8. https:// doi.org/10.1038/s41564-018-0187-6 PMID: 29988048

33. Bandini G, Damerow S, Güther MLS, Mehlert A, Guo H, Beverley SM, Ferguson MAJ(2019) bioRxiv 726117; https://doi.org/10.1101/726117

34. Turnock D. C., and Ferguson M. A. (2007) Sugar nucleotide pools of Trypanosoma brucei, Trypanosoma cruzi, and Leishmania major. Eukaryot Cell 6, 1450–1463 https://doi.org/10.1128/EC.00175-07 PMID: 17557881

35. Pontes de Carvalho L. C., Tomlinson S., Vandekerckhove F., Bienen E. J., Clarkson A. B., Jiang M. S., Hart G. W., and Nussenzweig V. (1993) Characterization of a novel trans-sialidase of Trypanosoma brucei procyclic trypomastigotes and identification of procyclin as the main sialic acid acceptor. J Exp Med 177, 465–474 https://doi.org/10.1084/jem.177.2.465 PMID: 8426115

36. Engstler M., Reuter G., and Schauer R. (1993) The developmentally regulated trans-sialidase from Trypanosoma brucei sialylates the procyclic acidic repetitive protein. Mol Biochem Parasitol 61, 1–13 https://doi.org/10.1016/0166-6851(93)90153-o PMID: 8259122

37. Doering T. L., Masterson W. J., Englund P. T., and Hart G. W. (1989) Biosynthesis of the glycosyl phosphatidylinositol membrane anchor of the trypanosome variant surface glycoprotein. Origin of the non-acetylated glucosamine. J Biol Chem 264, 11168–11173 PMID: 2525555

38. Urbaniak M. D., Crossman A., Chang T., Smith T. K., van Aalten D. M., and Ferguson M. A. (2005) The N-acetyl-D-glucosaminylphosphatidylinositol De-N-acetylase of glycosylphosphatidylinositol biosynthesis is a zinc metalloenzyme. J Biol Chem 280, 22831–22838 https://doi.org/10.1074/jbc.M502402200 PMID: 15817455

39. Jones D. C., Mehlert A., Guther M. L., and Ferguson M. A. (2005) Deletion of the glucosidase II gene in Trypanosoma brucei reveals novel N-glycosylation mechanisms in the biosynthesis of variant surface glycoprotein. J Biol Chem 280, 35929–35942 https://doi.org/10.1074/jbc.M509130200 PMID: 16120601

40. Bullard W, Lopes da Rosa-Spiegler J, Liu S, Wang Y, Sabatini R. Identification of the glucosyltransferase that converts hydroxymethyluracil to base J in the trypanosomatid genome. J Biol Chem. 2014; 289 (29):20273–82. https://doi.org/10.1074/jbc.M114.579821 PMID: 24891501

41. Roper J. R., Guther M. L., Milne K. G., and Ferguson M. A. (2002) Galactose metabolism is essential for the African sleeping sickness parasite Trypanosoma brucei. Proc Natl Acad Sci U S A 99, 5884–5889 https://doi.org/10.1073/pnas.092669999 PMID: 11983889

42. Bandini G., Marino K., Guther M. L., Wernimont A. K., Kuettel S., Qiu W., Afzal S., Kelner A., Hui R., and Ferguson M. A. (2012) Phosphoglucomutase is absent in Trypanosoma brucei and redundantly substituted by phosphomannomutase and phospho-N-acetylglucosamine mutase. Mol Microbiol 85, 513–534 https://doi.org/10.1111/j.1365-2958.2012.08124.x PMID: 22676716

43. Shaw M. P., Bond C. S., Roper J. R., Gourley D. G., Ferguson M. A., and Hunter W. N. (2003) High-resolution crystal structure of Trypanosoma brucei UDP-galactose 4'-epimerase: a potential target for structure-based development of novel trypanocides. Mol Biochem Parasitol 126, 173–180 https://doi.org/10.1016/s0166-6851(02)00243-8 PMID: 12615316

44. Roper J. R., Guther M. L., Macrae J. I., Prescott A. R., Hallyburton I., Acosta-Serrano A., and Ferguson M. A. (2005) The suppression of galactose metabolism in procylic form Trypanosoma brucei causes cessation of cell growth and alters procyclin glycoprotein structure and copy number. J Biol Chem 280, 19728–19736 https://doi.org/10.1074/jbc.M502370200 PMID: 15767252

45. Marino K., Guther M. L., Wernimont A. K., Amani M., Hui R., and Ferguson M. A. (2010) Identification, subcellular localization, biochemical properties, and high-resolution crystal structure of Trypanosoma brucei UDP-glucose pyrophosphorylase. Glycobiology 20, 1619–1630 https://doi.org/10.1093/glycob/cwq115 PMID: 20724435

46. Kuettel S., Wadum M. C., Guther M. L., Marino K., Riemer C., and Ferguson M. A. (2012) The de novo and salvage pathways of GDP-mannose biosynthesis are both sufficient for the growth of bloodstream-form Trypanosoma brucei. Mol Microbiol 84, 340–351 https://doi.org/10.1111/j.1365-2958.2012.08026.x PMID: 22375793

47. Zmuda F, Shepherd SM, Ferguson MAJ, Gray DW, Torrie LS, De Rycker M. Trypanosoma cruzi Phosphomannomutase and Guanosine Diphosphate-Mannose Pyrophosphorylase Ligandability Assessment. Antimicrob Agents Chemother. 2019; 63(10). https://doi.org/10.1128/AAC.01082-19 PMID: 31405854

48. Denton H., Fyffe S., and Smith T. K. (2010) GDP-mannose pyrophosphorylase is essential in the bloodstream form of Trypanosoma brucei. Biochem J 425, 603–614 https://doi.org/10.1042/BJ20090896 PMID: 19919534

49. Marino K., Guther M. L., Wernimont A. K., Qiu W., Hui R., and Ferguson M. A. (2011) Characterization, localization, essentiality, and high-resolution crystal structure of glucosamine 6-phosphate N-acetyl-transferase from Trypanosoma brucei. Eukaryot Cell 10, 985–997 https://doi.org/10.1128/EC.05025-11 PMID: 21531872

50. Stokes M. J., Guther M. L., Turnock D. C., Prescott A. R., Martin K. L., Alphey M. S., and Ferguson M. A. (2008) The synthesis of UDP-N-acetylglucosamine is essential for bloodstream form trypanosoma brucei in vitro and in vivo and UDP-N-acetylglucosamine starvation reveals a hierarchy in parasite protein glycosylation. J Biol Chem 283, 16147–16161 https://doi.org/10.1074/jbc.M709581200 PMID: 18381290

51. Urbaniak M. D., Collie I. T., Fang W., Aristotelous T., Eskilsson S., Raimi O. G., Harrison J., Navratilova I. H., Frearson J. A., van Aalten D. M., and Ferguson M. A. (2013) A novel allosteric inhibitor of the uridine diphosphate N-acetylglucosamine pyrophosphorylase from Trypanosoma brucei. ACS Chem Biol 8, 1981–1987 https://doi.org/10.1021/cb400411x PMID: 23834437

52. Turnock D. C., Izquierdo L., and Ferguson M. A. (2007) The de novo synthesis of GDP-fucose is essential for flagellar adhesion and cell growth in Trypanosoma brucei. J Biol Chem 282, 28853–28863 https://doi.org/10.1074/jbc.M704742200 PMID: 17640865

53. Colasante C, Ellis M, Ruppert T, Voncken F. Comparative proteomics of glycosomes from bloodstream form and procyclic culture form Trypanosoma brucei brucei. Proteomics. 2006; 6(11):3275–93. https://doi.org/10.1002/pmic.200500668 PMID: 16622829

54. Guther ML, Urbaniak MD, Tavendale A, Prescott A, Ferguson MA. High-confidence glycosome proteome for procyclic form Trypanosoma brucei by epitope-tag organelle enrichment and SILAC proteomics. J Proteome Res. 2014; 13(6):2796–806. https://doi.org/10.1021/pr401209w PMID: 24792668

55. Opperdoes F. R., and Borst P. (1977) Localization of nine glycolytic enzymes in a microbody-like organelle in Trypanosoma brucei: the glycosome. FEBS Lett 80, 360–364 https://doi.org/10.1016/0014-5793(77)80476-6 PMID: 142663

56. Opperdoes F. R., Baudhuin P., Coppens I., De Roe C., Edwards S. W., Weijers P. J., and Misset O. (1984) Purification, morphometric analysis, and characterization of the glycosomes (microbodies) of the protozoan hemoflagellate Trypanosoma brucei. J Cell Biol 98, 1178–1184 https://doi.org/10.1083/jcb.98.4.1178 PMID: 6715405

57. Aman R. A., and Wang C. C. (1986) An improved purification of glycosomes from the procyclic trypomastigotes of Trypanosoma brucei. Mol Biochem Parasitol 21, 211–220 https://doi.org/10.1016/0166-6851(86)90126-x PMID: 3807943

58. Heise N., and Opperdoes F. R. (1999) Purification, localisation and characterisation of glucose-6-phosphate dehydrogenase of Trypanosoma brucei. Mol Biochem Parasitol 99, 21–32 https://doi.org/10.1016/s0166-6851(98)00176-5 PMID: 10215021

59. Visser N., and Opperdoes F. R. (1980) Glycolysis in Trypanosoma brucei. Eur J Biochem 103, 623–632 https://doi.org/10.1111/j.1432-1033.1980.tb05988.x PMID: 6766864

60. Joice A.C., Lyda T.L., Sayce A.C., Verplaetse E., Morris M.T., Michels P.A., et al. Extra-glycosomal localisation of Trypanosoma brucei hexokinase 2. Int J Parasitol. 2012; 42(4):401–9. https://doi.org/10.1016/j.ijpara.2012.02.008 PMID: 22619756

61. Morris MT, DeBruin C, Yang Z, Chambers JW, Smith KS, Morris JC. Activity of a second Trypanosoma brucei hexokinase is controlled by an 18-amino-acid C-terminal tail. Eukaryot Cell. 2006; 5(12):2014–23. https://doi.org/10.1128/EC.00146-06 PMID: 17028241

62. Albert MA, Haanstra JR, Hannaert V, Van Roy J, Opperdoes FR, Bakker BM, et al. Experimental and in silico analyses of glycolytic flux control in bloodstream form Trypanosoma brucei. J Biol Chem. 2005; 280(31):28306–15. https://doi.org/10.1074/jbc.M502403200 PMID: 15955817

63. Chambers JW, Fowler ML, Morris MT, Morris JC. The anti-trypanosomal agent lonidamine inhibits Trypanosoma brucei hexokinase 1. Mol Biochem Parasitol. 2008; 158(2):202–7. https://doi.org/10.1016/j.molbiopara.2007.12.013 PMID: 18262292

64. Arsenieva D., Appavu B. L., Mazock G. H., and Jeffery C. J. (2009) Crystal structure of phosphoglucose isomerase from Trypanosoma brucei complexed with glucose-6-phosphate at 1.6 A resolution. Proteins 74, 72–80 https://doi.org/10.1002/prot.22133 PMID: 18561188

65. Opperdoes F. R., and Szikora J. P. (2006) In silico prediction of the glycosomal enzymes of Leishmania major and trypanosomes. Mol Biochem Parasitol 147, 193–206 https://doi.org/10.1016/j.molbiopara.2006.02.010 PMID: 16546274

66. Gualdron-Lopez M., Brennand A., Hannaert V., Quinones W., Caceres A. J., Bringaud F., Concepcion J. L., and Michels P. A. (2012) When, how and why glycolysis became compartmentalised in the

Kinetoplastea. A new look at an ancient organelle. Int J Parasitol 42, 1–20 https://doi.org/10.1016/j.ijpara.2011.10.007 PMID: 22142562

67. Haanstra J. R., Gonzalez-Marcano E. B., Gualdron-Lopez M., and Michels P. A. (2016) Biogenesis, maintenance and dynamics of glycosomes in trypanosomatid parasites. Biochim Biophys Acta 1863, 1038–1048 https://doi.org/10.1016/j.bbamcr.2015.09.015 PMID: 26384872

68. Allmann S., and Bringaud F. (2017) Glycosomes: A comprehensive view of their metabolic roles in T. brucei. Int J Biochem Cell Biol 85, 85–90 https://doi.org/10.1016/j.biocel.2017.01.015 PMID: 28179189

69. Galland N, Demeure F, Hannaert V, Verplaetse E, Vertommen D, Van der Smissen P, et al. Characterization of the role of the receptors PEX5 and PEX7 in the import of proteins into glycosomes of Trypanosoma brucei. Biochim Biophys Acta. 2007; 1773(4):521–35. https://doi.org/10.1016/j.bbamcr.2007.01.006 PMID: 17320990

70. Steiger RF, Opperdoes FR, Bontemps J. Subcellular fractionation of Trypanosoma brucei bloodstream forms with special reference to hydrolases. Eur J Biochem. 1980; 105(1):163–75. https://doi.org/10.1111/j.1432-1033.1980.tb04486.x PMID: 6245876

71. Ammerman ML, Hashimi H, Novotna L, Cicova Z, McEvoy SM, Lukes J, Read LK. 2011. MRB3010 is a core component of the MRB1 complex that facilitates an early step of the kinetoplastid RNA editing process. RNA 17:865–877. https://doi.org/10.1261/rna.2446311 PMID: 21451155

72. Van Veldhoven PP, Baumgart E, Mannaerts GP. Iodixanol (Optiprep), an improved density gradient medium for the iso-osmotic isolation of rat liver peroxisomes. Anal Biochem. 1996; 237(1):17–23. https://doi.org/10.1006/abio.1996.0194 PMID: 8660531

73. Penha LL, Sant'Anna CB, Mendonca-Previato L, Cunha-e-Silva NL, Previato JO, Lima AP. Sorting of phosphoglucomutase to glycosomes in Trypanosoma cruzi is mediated by an internal domain. Glycobiology. 2009; 19(12):1462–72. https://doi.org/10.1093/glycob/cwp121 PMID: 19696235

74. Galland N, de Walque S, Voncken FG, Verlinde CL, Michels PA. An internal sequence targets Trypanosoma brucei triosephosphate isomerase to glycosomes. Mol Biochem Parasitol. 2010; 171(1):45–9. https://doi.org/10.1016/j.molbiopara.2010.01.002 PMID: 20138091

75. Titorenko VI, Nicaud JM, Wang H, Chan H, Rachubinski RA. Acyl-CoA oxidase is imported as a heteropentameric, cofactor-containing complex into peroxisomes of Yarrowia lipolytica. J Cell Biol. 2002; 156 (3):481–94. https://doi.org/10.1083/jcb.200111075 PMID: 11815635

76. Crozier TWM, Tinti M, Larance M, Lamond AI, Ferguson MAJ. Prediction of Protein Complexes in Trypanosoma brucei by Protein Correlation Profiling Mass Spectrometry and Machine Learning. Mol Cell Proteomics. 2017; 16(12):2254–67. https://doi.org/10.1074/mcp.O117.068122 PMID: 29042480

77. Bauer S, Morris MT. Glycosome biogenesis in trypanosomes and the de novo dilemma. PLoS Negl Trop Dis. 2017; 11(4):e0005333. https://doi.org/10.1371/journal.pntd.0005333 PMID: 28426655

78. Bauer ST, McQueeney KE, Patel T, Morris MT. Localization of a Trypanosome Peroxin to the Endoplasmic Reticulum. J Eukaryot Microbiol. 2017; 64(1):97–105. https://doi.org/10.1111/jeu.12343 PMID: 27339640

79. Bauer S, Morris JC, Morris MT. Environmentally regulated glycosome protein composition in the African trypanosome. Eukaryot Cell. 2013; 12(8):1072–9. https://doi.org/10.1128/EC.00086-13 PMID: 23709182

80. Dean S, Sunter JD, Wheeler RJ. TrypTag.org: A Trypanosome Genome-wide Protein Localisation Resource. Trends Parasitol. 2017; 33(2):80–2. https://doi.org/10.1016/j.pt.2016.10.009 PMID: 27863903

81. Liu L, Xu YX, Caradonna KL, Kruzel EK, Burleigh BA, Bangs JD, et al. Inhibition of nucleotide sugar transport in Trypanosoma brucei alters surface glycosylation. J Biol Chem. 2013; 288(15):10599–615. https://doi.org/10.1074/jbc.M113.453597 PMID: 23443657

82. Brun R, Schonenberger M. Cultivation and in vitro cloning or procyclic culture forms of Trypanosoma brucei in a semi-defined medium. Short communication. Acta Trop. 1979; 36(3):289–92. PMID: 43092

83. Greig N, Wyllie S, Patterson S, Fairlamb AH. A comparative study of methylglyoxal metabolism in trypanosomatids. FEBS J. 2009; 276(2):376–86. https://doi.org/10.1111/j.1742-4658.2008.06788.x PMID: 19076214

84. Dunn KW, Kamocka MM, McDonald JH. A practical guide to evaluating colocalization in biological microscopy. Am J Physiol Cell Physiol. 2011; 300(4):C723–42. https://doi.org/10.1152/ajpcell.00462.2010 PMID: 21209361

85. Cox J, Mann M. MaxQuant enables high peptide identification rates, individualized p.p.b.-range mass accuracies and proteome-wide protein quantification. Nat Biotechnol. 2008; 26(12):1367–72. https://doi.org/10.1038/nbt.1511 PMID: 19029910

86. Tyanova S, Temu T, Cox J. The MaxQuant computational platform for mass spectrometry-based shotgun proteomics. Nat Protoc. 2016; 11(12):2301–19. https://doi.org/10.1038/nprot.2016.136 PMID: 27809316

87. Cox J, Neuhauser N, Michalski A, Scheltema RA, Olsen JV, Mann M. Andromeda: a peptide search engine integrated into the MaxQuant environment. J Proteome Res. 2011; 10(4):1794–805. https://doi.org/10.1021/pr101065j PMID: 21254760

88. Aslett M, Aurrecoechea C, Berriman M, Brestelli J, Brunk BP, Carrington M, et al. TriTrypDB: a functional genomic resource for the Trypanosomatidae. Nucleic Acids Res. 2010; 38(Database issue): D457–62. https://doi.org/10.1093/nar/gkp851 PMID: 19843604

89. Sury MD, Chen JX, Selbach M. The SILAC fly allows for accurate protein quantification in vivo. Mol Cell Proteomics. 2010; 9(10):2173–83. https://doi.org/10.1074/mcp.M110.000323 PMID: 20525996

90. Cox J, Matic I, Hilger M, Nagaraj N, Selbach M, Olsen JV, et al. A practical guide to the MaxQuant computational platform for SILAC-based quantitative proteomics. Nat Protoc. 2009; 4(5):698–705. https://doi.org/10.1038/nprot.2009.36 PMID: 19373234

91. Perez-Riverol Y, Csordas A, Bai J, Bernal-Llinares M, Hewapathirana S, Kundu DJ, et al. The PRIDE database and related tools and resources in 2019: improving support for quantification data. Nucleic Acids Res. 2019; 47(D1):D442–D450. https://doi.org/10.1093/nar/gky1106 PMID: 30395289